Atmospheric Pollution Research 11 (2020) 1281–1289

HOSTED BY

Contents lists available at ScienceDirect

Atmospheric Pollution Research

journal homepage: www.elsevier.com/locate/apr

Spatial distribution and source contributions of $PM_{2.5}$ concentrations in Jincheng, China

Dongpeng Guo, Ran Wang*, Peng Zhao

College of Environment and Safety, Taiyuan University of Science and Technology, Taiyuan, China

ARTICLE INFO

Keywords:
$PM_{2.5}$
WRF
CALPUFF
Spatial distribution
Concentration contribution

ABSTRACT

This study investigates the spatial distribution and source contributions of fine particles ($PM_{2.5}$) in complex terrain in Jincheng, China, using the Weather Research and Forecast (WRF) Model/California Puff Model (CALPUFF) modeling system. To evaluate the CALPUFF performance, the simulated results were compared with the observational data at the three monitoring stations. The results show that the CALPUFF simulation results underestimate the daily average concentration of $PM_{2.5}$, and the statistical analysis also reveals an underestimation trend. The spatial distribution shows that $PM_{2.5}$ concentrations decrease gradually outward from the Jincheng city center. Primary $PM_{2.5}$ concentrations in December are significantly higher than those in July. However, the concentrations of secondary sulfate ions (SO_4^{2-}) and nitrate ions (NO_3^-) in July are higher than those in December. In December, residential heating was the main contributor to the $PM_{2.5}$ concentration, accounting for 50%, and industrial processes and dust (an anthropogenic dust from construction processes, open yards and roads) accounted for 18% and 14%, respectively.

1. Introduction

With population growth and the rapid process of urbanization, air pollution problems have been inevitable all around the world. Air pollutants may affect the health of humans and animals (Ozkurt et al., 2013; Mardones and Saavedra, 2016; Tartakovsky et al., 2016,Tartakovsky et al., 2016). $PM_{2.5}$ is a fine dust pollutant with an aerodynamic diameter smaller than 2.5 μm (Liu et al., 2019; Jain et al., 2007). $PM_{2.5}$ can be further divided into primary and secondary fine particles. Primary fine particles are emitted directly into the atmosphere from factories while secondary fine particles are formed in the ambient air by chemical reactions (Zhou et al., 2003; Jain et al., 2007; Arunachalam et al., 2011). $PM_{2.5}$ is mainly caused by anthropogenic emissions, such as fossil fuel combustion and industrial production processes (Levy et al., 2002; Yang et al., 2019,Yang et al., 2019). In 2006, the Word Health Organization estimated many diseases (such as cardiovascular and respiratory diseases) in populations in developing countries are due to exposure to $PM_{2.5}$ (WHO et al., 2006). $PM_{2.5}$ pollution has become a worldwide concern, especially in China (Wang et al., 2019; Yang et al., 2019,Yang et al., 2019; Zhou et al., 2006).

Air quality models have proven useful in determining the spatial distribution of air pollutants and for developing emission control policies that reduce emissions of air pollutants (Lee et al., 2014). Commonly used air quality models include the Industrial Source Complex 3 (ISC3) model, the Atmospheric Dispersion Modeling System (ADMS), the AMS/EPA Regulatory Model (AERMOD) and CALPUFF. ISC3 is used to simulate the dispersion of primary pollutants in simple terrain where the terrain height (excluding buildings) within 5 km of the center of the pollution source is lower than the height of the exhaust pipe (Hanna et al., 2001). Compared with ISC3, ADMS and AERMOD have the state-of-the-art algorithm for turbulent dispersion, and they can simulate the dispersion of pollutants in complex terrain (Kalhor and Bajoghli, 2017). The above three models usually assume steady state, straight-line transport of pollutants in time and space, and their simulation range is generally less than 50 km; the performance becomes worst in the far field. However, this assumption is inappropriate because the wind field is inhomogeneous in a complex terrain. CALPUFF can model atmospheric pollutants for long-range transport (more than 50 km) (CALPUFF Dispersion Model, 2000) in complex terrains, because it can handle complex three-dimensional wind fields (Nagendra et al., 2016). The CALPUFF model is a regulatory model recommended by the U.S. Environmental Protection Agency (USEPA) and is widely used in many countries. In addition to calculating pollutant concentrations in air, the CALPUFF model can also simulate plume dispersion and particle deposition under both dry and wet conditions (Scire et al., 2000; Macintosh et al., 2010).

Peer review under responsibility of Turkish National Committee for Air Pollution Research and Control.
* Corresponding author. College of Environment and Safety, Taiyuan University of Science and Technology, Waliu Road 66, Taiyuan, 030024, China.
E-mail address: RWang1996@126.com (R. Wang).

https://doi.org/10.1016/j.apr.2020.05.004
Received 9 December 2019; Received in revised form 1 May 2020; Accepted 3 May 2020
Available online 05 May 2020

The CALPUFF model is widely used to simulate the atmospheric transport of pollutants. Abdul-Wahab et al. (2018) used CALPUFF to model the dispersion in an atmosphere of sulfur dioxide (SO_2), nitrogen dioxides (NO_x), carbon monoxide (CO), and particulate matter with a diameter of less than 10 μm (PM_{10}) from a steel plant located in Muscat, Oman in winter and summer. Abdul-Wahab and Fadlallah (2014) investigated the dispersion of three typical vehicle emissions (CO, NO_x, and carbon dioxide (CO_2)) in Muscat, Oman, using CALPUFF software. In addition, some researchers analyzed the source contribution of pollutants based on the CALPUFF model. Li and Xie (2016) applied the CALPUFF model to simulate the spatial distribution of SO_2 in Urumqi, China and analyzed the source contribution to areas where the SO_2 concentration is high. Yim et al. (2010) employed the CALPUFF model to simulate the atmospheric distribution and concentration of SO_2 from some emission sources in different regions of the Hong Kong Special Administrative Region (HKSAR). Murena et al. (2018) calculated the contribution of nitrogen dioxide (NO_2) and SO_2 emitted by cruise ships in the Gulf of Naples. Yates et al. (2017) and Pivato et al. (2015) used the CALPUFF model to investigate the effects of pesticides on humans and soil, respectively. CALPUFF was used to model odor dispersion from municipal solid waste treatment plants and pig farms (Ranzato et al., 2012; Cai et al., 2015; Melo et al., 2012). Many studies have validated CALPUFF predictions. Holnicki et al. (2016) used the CALPUFF model to simulate the concentrations of PM_{10}, $PM_{2.5}$, NO_x, SO_2, CO, and benzene (C_6H_6) in the Warsaw Metropolitan Area. The results showed that the good performance of the model is achieved for the annual mean predictions, whereas the temporal agreement in the short-term, 1-h average concentrations is much less accurate, especially under low-wind meteorological conditions. Cui et al. (2011) validated the application of the CALPUFF model for the near-field dispersion of short-term emission sources in complex terrain, and found that the model underestimates predictions, especially in peak concentrations.

The simulated results of the secondary pollutant in the CALPUFF simulation are uncertain due to the limitations of the model algorithms in chemical transformations (US EPA, 1998). Mangia et al. (2015) estimated the long-term exposure of $PM_{2.5}$ for a power plant and noted some limitations of the study, including gas-particle conversion as a non-linear chemical process; the CALPUFF model uses a simplified linear mechanism, and the background concentrations of ammonia (NH_3) and ozone (O_3) also affect the $PM_{2.5}$ concentrations. Lopez et al. (2005) evaluated the human health impacts of $PM_{2.5}$ from one of Mexico's largest power plants. The results showed that the chemical mechanism choice in the CALPUFF model has little effect on secondary PM2.5 concentrations.

This paper integrates the mesoscale weather forecasting model WRF with the CALPUFF model to simulate $PM_{2.5}$ (including primary $PM_{2.5}$ and secondary $PM_{2.5}$) concentrations in Jincheng in July and December 2017. The reliability of the CALPUFF model was validated by comparing simulated concentrations with monitoring data. In addition, the spatial distribution and source contributions of $PM_{2.5}$ in Jincheng were analyzed.

2. Methodology

2.1. Study area and pollutant source description

Jincheng is a city in southeastern Shanxi Province, China (35°11′-36°04′ N, 111°55′-113°37′ E), and the population of the whole Jincheng area is 2.333 million people. The east-west direction is approximately 160 km, the south-north direction is approximately 100 km, and its total area coverage is 9490 square kilometers. The location of Jincheng is shown in Fig. 1. The whole area is similar to a dustpan with a relatively complex terrain setting, and the altitude in the northern area is high, the altitude in the southern and central areas is low. The average elevation of Jincheng city is 600–700 m, and the highest elevation is 2322 m while the lowest elevation is close to 300 m.

There are numerous industrial sources (mining, steel, cement, coking) of air pollutants in Jincheng. Table 1 shows the emission data for various industrial activities, and the emission data from Jincheng's 2017 pollution source emission inventory (Jincheng Environmental Protection Department, 2017). As we can see, residential heating emits much SO_2, NO_X and $PM_{2.5}$, and the emission data for each of 6 regions is shown in Table 2. Power plants and industrial boilers emit large amounts of SO_2 and NO_x every year. Vehicles emit a small amount of $PM_{2.5}$, and the information on the line sources of transportation systems in emission inventory is missing. Therefore, vehicle exhaust emissions are not considered in our study, and $PM_{2.5}$ from other regions is not considered here due to a lack of data. We only studied the contribution of industrial and domestic sources of local $PM_{2.5}$. The sources for which the stack height is greater than 70 m or the boiler steam tonnage is greater than 120 t/h are regarded as point sources (see Fig. 1), while others are regarded as area sources. The regions indicated in Fig. 1 are regarded as area sources, including Qinshui, Gaoping, Lingchuan, Yangcheng, Zezhou and urban area. Therefore, in total, 80 point sources and 6 area sources were used in the simulation. Table 3 shows the area source emission data. Zezhou emits more $PM_{2.5}$ than other regions. Most industrial activities operate year-round, so we assumed the same release of pollutants in July and December, excluding residential heating. For residential heating, we used the emission rate in summer to simulate the $PM_{2.5}$ concentrations in July, and used the emission rate in winter to simulate the $PM_{2.5}$ concentrations in December. The emissions from residential heating are estimated by multiplying the emission rates and relevant activity data.

2.2. Model description

In this paper, the WRF/CALPUFF modeling system is used to investigate the spatial distribution and source contributions of $PM_{2.5}$ concentrations in Jincheng. WRF is the latest-generation mesoscale numerical weather prediction model and was developed by the National Center for Atmospheric Research (NCAR), the Pacific Northwest National Laboratory (PNNL) and the National Oceanic and Atmospheric Administration (NOAA) (WRF Modeling System User's guide, 2005). The outputs of the WRF model can provide meteorological fields to be used as input for air quality models such as CALPUFF. CALPUFF is a multi-layer, multi-species non-steady-state Lagrangian puff dispersion model that can simulate the effects of temporally and spatially varying meteorological conditions on pollutant transport, transformation, and removal. The CALPUFF model can consider plume rise, plume buoyancy, vertical wind shear, and atmospheric stability when calculating plume dispersion (Scire et al., 2000).

In this study, the WRF (WRFv3.6.1) model is used to generate a large-scale wind field as a first guess field in the meteorological model of CALPUFF (CALMET)(Tian et al., 2013). The initial conditions and boundary conditions for the WRF model are provided by the National Center for Environmental Prediction (NCEP) Final Analysis (FNL). The FNL fields were at 6-h intervals with a spatial resolution of 1° (approximately 111 km). The WRF model is configured with two nested domains, the horizontal resolution of the grids are 6 km and 3 km (see Fig. 1), and the height of vertical elevation includes 32 layers (up to 9000 m). Outputs from the inner domain were horizontally and vertically interpolated to the CALMET grids as an initial -guess wind field (see Fig. 1 D01). CALMET is a diagnostic wind field processor with micro-meteorological modules, it forms hourly wind and temperature fields. CALMET was configured with domain covering the whole of Jincheng city, the simulated domains were 200 × 125 (160 km × 100 km) grid cells with a resolution of 800 m and 10 layers which corresponded to the physical heights of 20 m, 40 m, 80 m, 160 m, 320 m, 640 m, 1200 m, 2000 m, 3000 m, 4000 m. Terrain data (spatial resolution: 90 m) (http://scr.com/calpuff/data/terrain.html) and land use data (spatial resolution: 1000 m) (http://scr.com/calpuff/data/land_use.html) were obtained from the United States Geological

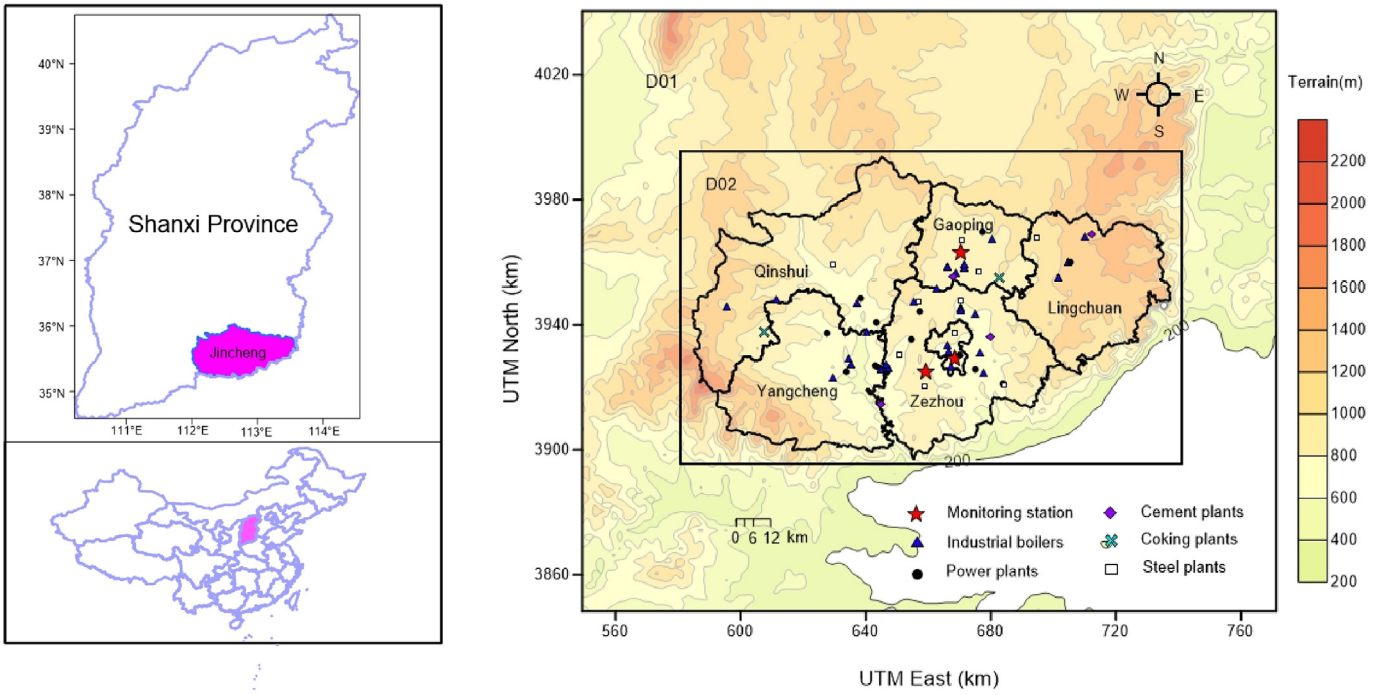

Fig. 1. Location of Jincheng and the distributions of point sources in Jincheng.

Table 1
The total emission data for sources.

Type	Number	SO_2(Tons/year)	NO_x(Tons/year)	$PM_{2.5}$(Tons/year)
Industrial boilers	297	4206	11712	1722
Power plants	35	4929	13241	248
Cement plants	12	718	1064	579
Coking plants	2	84	841	70
Steel plants	21	656	4395	1225
Dust				9298
Residential heating		26623	2116	15613
Vehicle exhaust		83	9024	251

Table 2
Residential heating emission data for each of 6 regions.

Season	Region	SO_2 (Tons/season)	NO_x(Tons/season)	$PM_{2.5}$(Tons/season)
Summer	Qinshui	281.23	21.90	165.07
	Gaoping	542.61	42.25	318.48
	Lingchuan	370.87	28.87	217.68
	Yangcheng	566.71	44.13	332.63
	Zezhou	827.88	64.46	485.92
	urban	71.36	5.56	41.88
Winter	Qinshui	1124.90	87.58	660.26
	Gaoping	2170.42	168.99	1273.94
	Lingchuan	1483.49	115.51	870.74
	Yangcheng	2266.84	176.50	1330.53
	Zezhou	3311.51	257.84	1943.70
	urban	285.44	22.22	167.54

Survey (USGS). The MESOPUFF II chemical transformation method was used in the CALPUFF simulation, including six pollutant species: SO_2, SO_4, NO_x, nitric acid (HNO_3), NO_3 and $PM_{2.5}$, where, SO_2 is oxidized by O_3 to SO_4^{2-}, NO_x is oxidized by O_3 to NO_3^- and organic nitrogen, and SO_4^{2-} and NO_3^- reacts with ammonia (NH_3) to form $(NH_4)_2SO_4$ and NH_4NO_3, respectively. In the chemical transformation method used by the CALPUFF model, the daytime SO_2 oxidation is an hourly varying

Table 3
Area source emission data.

Region	Area(km^2)	$PM_{2.5}$(Tons/year)
Qinshui	2676.6	2300
Gaoping	946	4580
Lingchuan	1751	2637
Yangcheng	1930.7	6872
Zezhou	2023	7241
urban	149.6	2961

function of background ozone concentration, solar radiation, atmospheric stability and relative humidity. Similarly, daytime NO_x oxidation is an hourly varying function of background ozone concentration and atmospheric stability. The nighttime oxidation rates of SO_2 and NO_x are assumed to be 0.2% and 2.0%, respectively (US EPA, 1998). The deposition of $PM_{2.5}$ in dry and wet conditions is also considered in this study. In addition, we selected puff sample function method, Pasquill-Gifford (PG) curves, Industrial Source Complex (ISC) rural curves and McElroy-Pooler (MP) coefficients (urban) to compute the dispersion of $PM_{2.5}$ (Tartakovsky et al., 2016,Tartakovsky et al., 2016; Tian et al., 2013). The SO_4^{2-} and NO_3^- concentrations output by MESOPUFF II are multiplied by factors of 1.374 and 1.29 to convert to ammonium sulfate ($(NH_4)_2SO_4$) and ammonium nitrate (NH_4NO_3), respectively (US EPA, 1998). Therefore, when calculating secondary $PM_{2.5}$ concentrations, we used $1.374SO_4^{2-}$ and $1.29NO_3^-$ to represent $(NH_4)_2SO_4$ and NH_4NO_3, respectively. The total $PM_{2.5}$ concentrations are equal to the sum of the concentrations of primary $PM_{2.5}$, 1.374 SO_4^{2-} and 1.29 NO_3^-.

3. Results and discussion

3.1. Validation of the CALPUFF model

To evaluate the performance of the CALPUFF model, the simulated concentrations were compared with the observational data from the monitoring stations in urban area (35.48°N, 112.84°E), Gaoping (35.81°N, 112.94°E) and Zezhou (35.38°N, 112.78°E) (shown in Fig. 1).

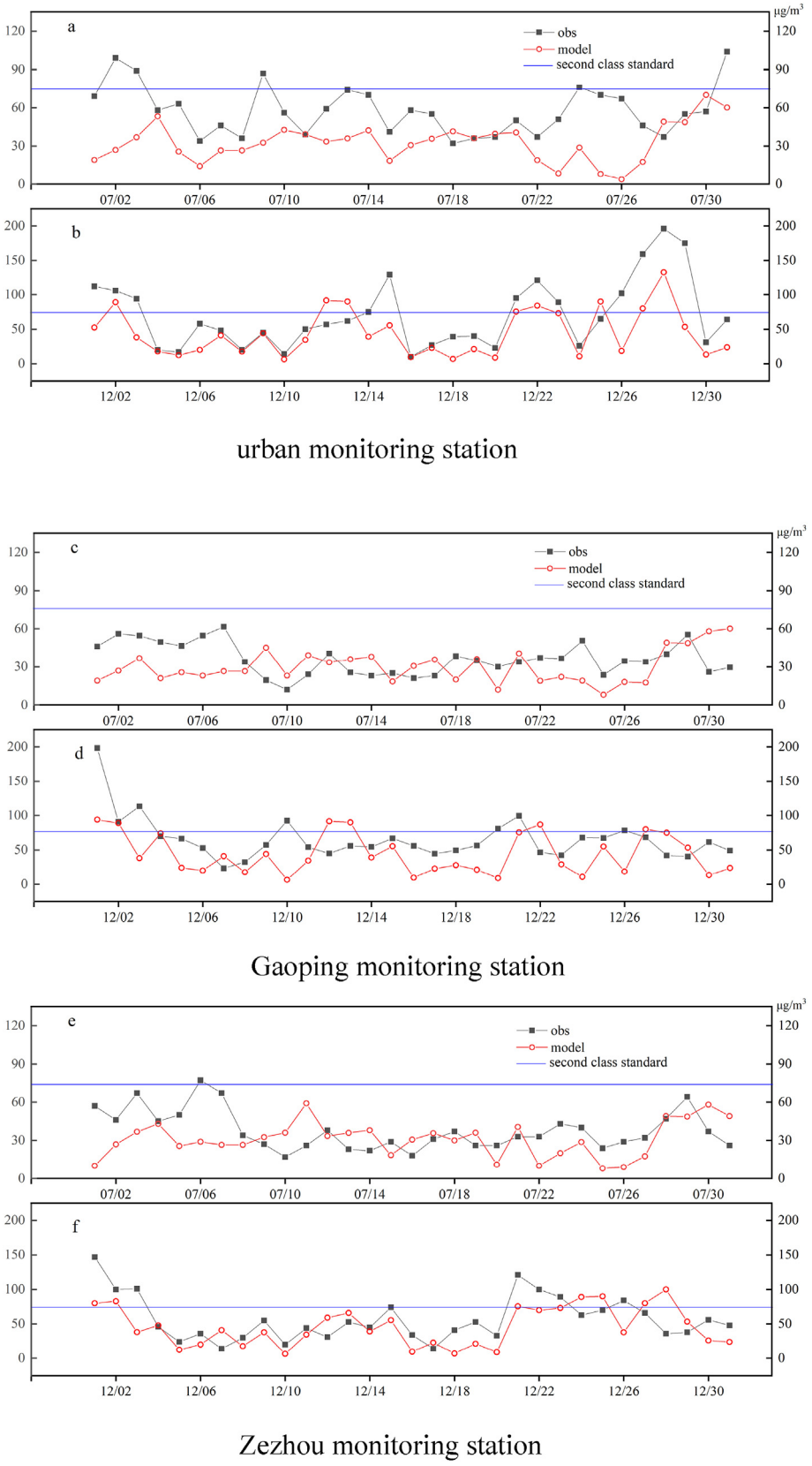

Fig. 2. Comparison of the simulated and observed daily average concentrations of $PM_{2.5}$ (a, c and e are the results of comparsion in July; b, d and f are the results of comparsion in December.).

The monitoring stations automatically record pollutants such as SO_2, NO_x, $PM_{2.5}$, and the acquisition rates of SO_2, NO_x and $PM_{2.5}$ are 0.65 L/min, 0.5 L/min and 16.7 L/min, respectively. The readings of SO_2, NO_x and $PM_{2.5}$ are recorded at intervals of 5- min, 5- min and 1 h, respectively. The hourly average concentrations of the air quality indicators are then computed accordingly, and finally, the daily average

concentrations are provided. In this paper, we used the daily average $PM_{2.5}$ concentrations to compare the discrepancy between the simulations and observations in July and December 2017. The National Air Quality Standard stipulates that the limit of daily average concentrations of $PM_{2.5}$ is 75 μg/m^3 (second-class standard). From Fig. 2, it can be seen that there are more days that exceed the second-class standard in December than in July. At the urban monitoring station, the simulated concentrations show a large underestimation in July, and the simulated concentrations are in good agreement with the observational data in December. At the Gaoping monitoring station, we can see that there are more days of underestimation than overestimation whether in July or in December. At the Zezhou monitoring station, the simulated concentrations in December are in a better agreement with the observed data than those in July. On the whole, the CALPUFF model underestimates the $PM_{2.5}$ concentrations. The discrepancy between the predictions and observations can be attributed to the following factors. First, our emission inventory does not include vehicle exhaust emissions, biomass burning, etc. Second, the impact of $PM_{2.5}$ from other regions on Jincheng is not considered in this study. Third, it is difficult for the model to reflect the real complex flow caused by mountainous land and rivers although the terrain effects are adjusted in CALMET (Cui et al., 2011).

To validate the reliability of the model, many researchers use statistical indicators to compare the discrepancy between the observations and predictions (Hoinaski et al., 2016; Choi et al., 2018; Rood, 2014). Five statistical indicators are used to verify the performance of the CALPUFF model: Factor of Two (FAC2), Geometric Variance (VG), Geometric Mean bias (MG), Fractional Bias (FB), and Normalized Mean Square Error (NMSE). The formulas used to derive these indicators are given in Equations (1)–(4) :

$$VG = \exp[\overline{\ln C_o - \ln Cp)^2}] \quad (1)$$

$$MG = \exp(\overline{\ln C_o} - \overline{\ln C_p}) \quad (2)$$

$$FB = \frac{\overline{C_o} - \overline{C_p}}{0.5(\overline{C_o} + \overline{C_p})} \quad (3)$$

$$NMSE = \frac{\overline{(C_p - Co)^2}}{\overline{C_p}\,\overline{C_o}} \quad (4)$$

where, C_o and C_p are the observed and predicted concentrations respectively, and $\overline{C_o}$ and $\overline{C_p}$ are the mean values over time for the predicted and observed concentrations, respectively. FAC2 is the most robust measure, and it is defined as the ratio of predictions within a factor of 2 of the observed values and can reflect the reliability of the simulated values (Hoinaski et al., 2016). VG may provide a more balanced treatment of extremely high and low values than the other metrics, and a perfect model performance would result in VG = 1 and MG = 1 (Rood, 2014). MG reflects the degree of bias in the geometric mean (Rood, 2014). FB is a linear measure, and reflects the degree of matching between the predicted and observed results; it ranges between −2 and +2, with a perfect model resulting in FB = 0 (Ghannam and El-Fadel, 2013). NMSE reflects the overall deviation between the simulated values and the observed values. The NMSE = 1 indicates that the predictions are equal to the observations (Ghannam and El-Fadel, 2013).

Table 4 gives the values of the statistical indicators at the three monitoring stations. The FAC2 value is 64.5% in July and 77.4% in December for the urban monitoring station. The FAC2 value is 58.1% in July and 74.2% in December for the Gaoping monitoring station. The FAC2 value is 83.9% in July and 90.3% in December for the Zezhou monitoring station. The scatter plots of the individual results are shown in Fig. 3. It can be seen that there are more underestimations than overestimations. Rood (2014) used the Winter Validation Tracer Study dataset to evaluate the performance of the AERMOD, Industrial Source Complex 2 (ISC2), CALPUFF and Regional Atmospheric Transport Code for Hanford Emission Tracking (RATCHET) models under the same conditions near Denver, Colorado. The results showed that the FAC2 and VG values for the CALPUFF model ranged from 0.58 to 0.917 and 1.5 to 2.5, respectively. The values of FAC2 and VG in our study are close to those reported by Rood (2014). The MG values at the three monitoring stations indicate that the simulated values are less than the observed values. The MG values in our study are closer to 1 than those reported by Ghannam and El-Fadel (2013). The FB values at the three monitoring stations both underpredict the observed values. Lee et al. (2014) used the CALPUFF model to simulate the concentrations of PM_{10} and SO_2 in two industrial complexes. In our study, the FB and NMSE values are within those reported by Lee et al. (2014). Overall, these statistical indicators show an underestimation trend.

Table 4
Statistical analysis of CALPUFF simulation results.

Monitoring station	Period	FAC2	VG	MG	FB	NMSE
urban	July	64.5%	2.507	1.944	0.556	0.615
	December	77.4%	1.730	1.680	0.451	0.590
Gaoping	July	58.1%	1.494	1.237	0.183	0.362
	December	74.2%	2.757	1.754	0.384	0.608
Zezhou	July	83.9%	1.621	1.284	0.198	0.386
	December	90.3%	2.592	1.446	0.254	0.584

3.2. Spatial distribution of $PM_{2.5}$ concentrations

The spatial distribution of pollutant concentrations is very important to obtain insight into regional environmental quality and to decide upon emission reduction measures.

The dispersion and distribution of pollutant concentrations are influenced by meteorological conditions. Specifically, wind direction and wind speed can affect the dispersion of pollutants. Fig. 4 shows that windrose plots at the urban monitoring station in July and December. As it can be seen that the prevailing wind directions are north, south and southeast winds in July, and the prevailing wind directions are north, south and northwest winds in December. The average wind speed in July is stronger than that in December, and there are some differences between the simulated and observed wind fields.

To define the peak of the spatial distributions of the $PM_{2.5}$ concentrations in July and December, the highest 24-h concentrations are used in our paper. Fig. 5 shows the spatial distributions of the primary $PM_{2.5}$, secondary SO_4^{2-} and NO_3^- concentrations in Jincheng. The concentration unit is μg/m^3 which represents the amount of $PM_{2.5}$ per cubic meter. From Fig. 5, it can be seen that in most areas of Jincheng, the range of the highest 24-h primary $PM_{2.5}$ concentrations is 15–120 μg/m^3 in July and 15–240 μg/m^3 in December, respectively. Overall, the primary $PM_{2.5}$ concentrations in December are higher than those in July mainly because of primary $PM_{2.5}$ emissions from coal-fired heating equipment in December (Sari and Bayram, 2014). In addition, temperature inversion easily occurs in winter, and it suppresses the dispersion of primary $PM_{2.5}$. The concentrations of secondary SO_4^{2-} and NO_3^- in July are higher than those in December probably because O_3 concentrations are relatively high in summer, which causes more NO_x and SO_2 gaseous precursors to be converted into secondary SO_4^{2-} and NO_3^-. Generally, more secondary particles are formed due to the higher oxidizing power of the atmosphere (Zhou et al., 2003).

The concentrations of primary $PM_{2.5}$ decrease gradually outward from the Jincheng city center. The concentration dispersion plumes of primary $PM_{2.5}$ reach beyond the modeling domain, which would increase the $PM_{2.5}$ pollution in other regions. Primary $PM_{2.5}$ concentrations are high at the junction of Zezhou, Qinshui and Gaoping. There are many factories that emit a great deal of primary $PM_{2.5}$. Primary $PM_{2.5}$ concentrations are the lowest in Lingchuan. For secondary SO_4^{2-} concentrations, high-concentration areas are small. Secondary NO_3^- concentrations are the highest in urban area, and secondary NO_3^-

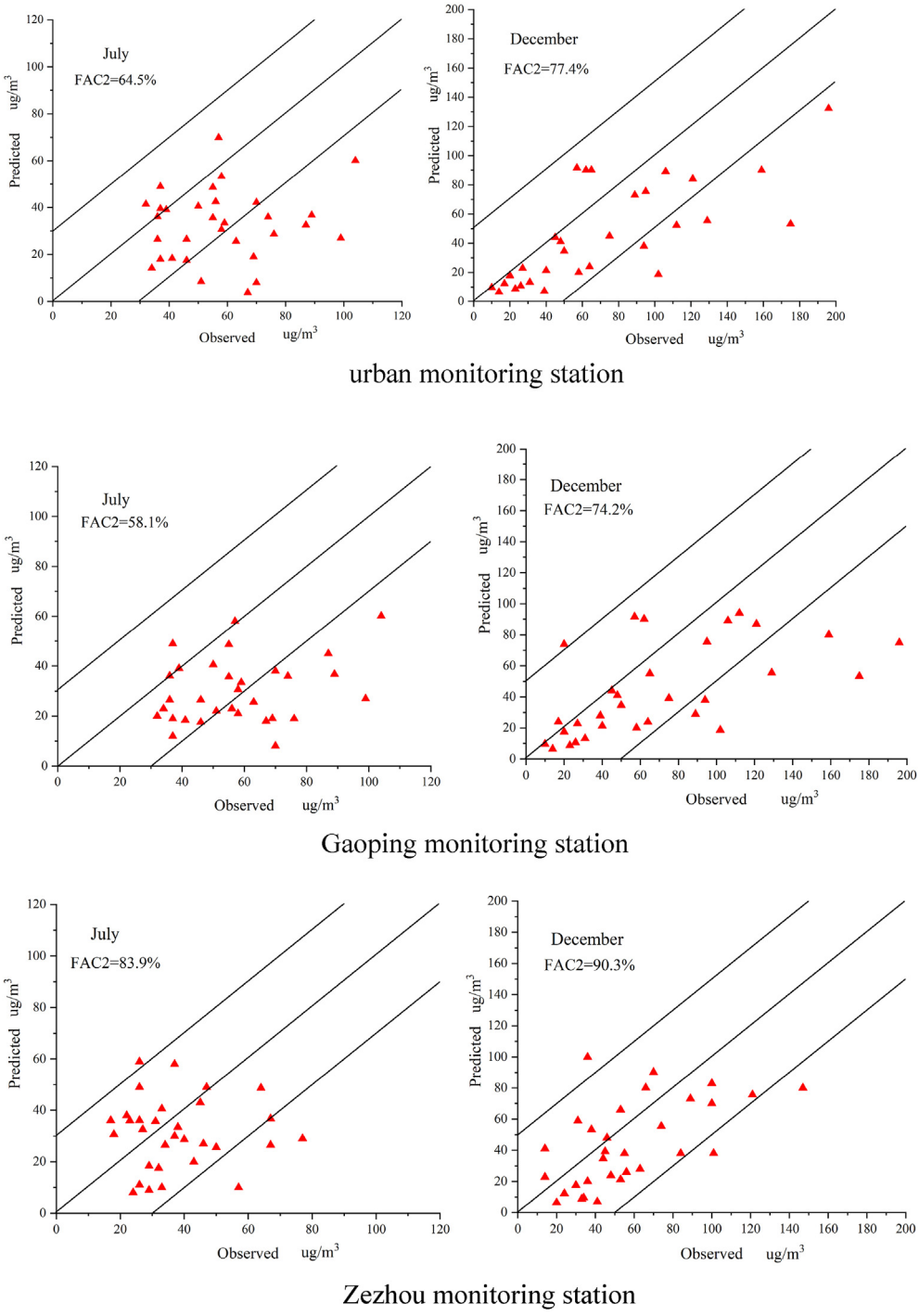

Fig. 3. The scatter plots of simulation results in three monitoring stations.

concentrations are high in Zezhou and Gaoping. Secondary NO_3^- concentrations are much higher than secondary SO_4^{2-} concentrations. The main reason is that NO_x source emissions are much higher than those of SO_2 in most plants. In addition, the transformation rate of NO_x is greater than that of SO_2.

3.3. Analysis of the concentration contribution of sources

To determine the $PM_{2.5}$ concentration contribution of various industrial activities, the daily average concentration of $PM_{2.5}$ in December was analyzed in this study (Yim et al., 2010). Each industrial activity may be divided into two parts: point sources and area sources. The daily average concentration of each industrial activity is the sum of the daily average concentration of point sources and area sources, and the ratio of the daily average concentration of $PM_{2.5}$ for each industrial activity can be calculated. The contribution of each industrial activity to the 24-h average concentrations of the total $PM_{2.5}$, primary $PM_{2.5}$, secondary SO_4^{2-} and NO_3^- are shown in Fig. 6. The concentration contribution of residential heating is the largest for the total $PM_{2.5}$ concentration in December, accounting for 50%. Jincheng is located in northern China, and much $PM_{2.5}$ and SO_2 are emitted because residents use coal-fired equipment for heating in winter. Furthermore, the height of stacks of coal-fired equipment are usually low, resulting in severe $PM_{2.5}$ pollution near the ground. The concentration contributions of

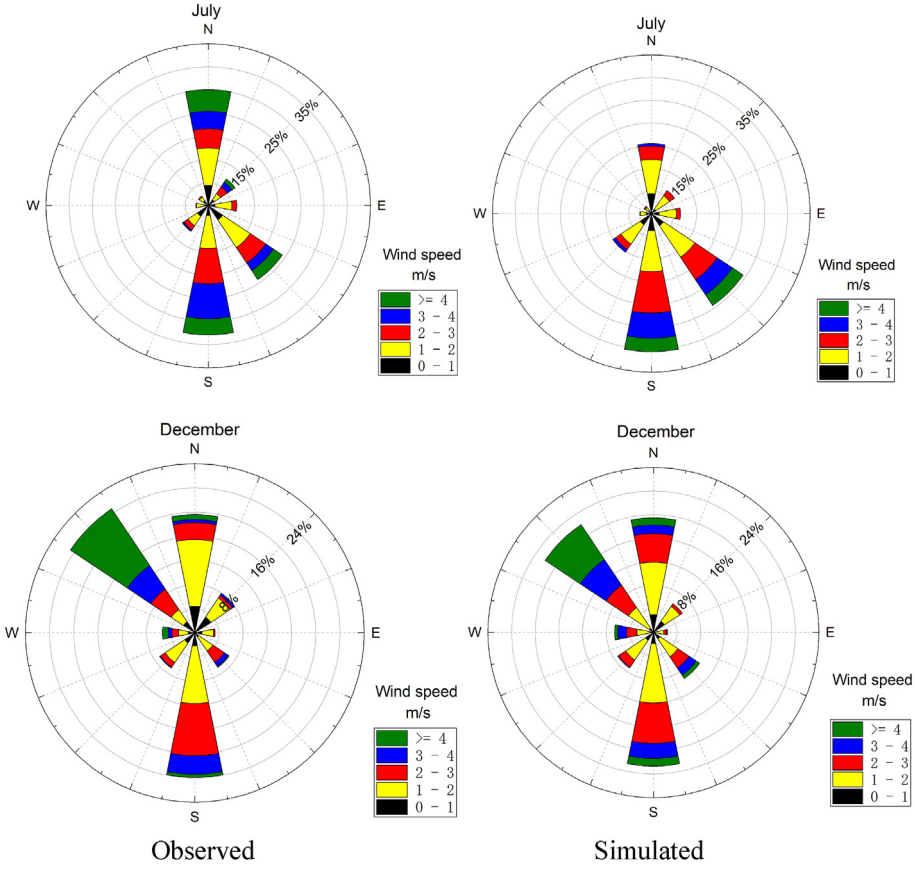

Fig. 4. Windrose plots at the urban monitoring station in July and December.

industrial processes and dust greatly contribute to the total $PM_{2.5}$ concentration, accounting for 18% and 14%, respectively. Industrial boilers, power plants and steel plants account for 6%, 3% and 2%, respectively, and they are not negligible for $PM_{2.5}$ pollution. The concentration contribution of residential heating is the largest for primary $PM_{2.5}$, accounting for 53%. The concentration contributions of industrial processes and dust account for 19% and 15%, respectively. The concentration contribution of residential heating is the highest for secondary SO_4^{2-}, accounting for 62%. The concentration contributions of power plants and industrial boilers are high, accounting for 11% and 9%, respectively. Power plants and industrial boilers are the main contributors of secondary NO_3^-, accounting for 33% and 32%, respectively, because of the large amount of NO_x generated in their daily operations. In conclusion, residential heating, industrial processes and dust significantly contribute to the $PM_{2.5}$ concentrations. Much $PM_{2.5}$, SO_2 and NO_x were emitted by human activities which caused high $PM_{2.5}$ concentrations. It is worth noting that the above analysis of the $PM_{2.5}$ concentration contribution is not completely accurate due to the limitations of the source inventory (our emission inventory does not include vehicle exhaust emissions, biomass burning, etc.), but it could be beneficial for the reduction in $PM_{2.5}$ emissions.

4. Conclusions

Air quality models are used to simulate the dispersion and physicochemical processes of air pollutants based on mathematical methods and meteorological theory. They can determine the spatial distribution of pollutants and can be used to develop the control measures for air quality.

In this study, the WRF/CALPUFF modeling system was used to simulate the spatial distribution and source contributions of the $PM_{2.5}$ concentrations in Jincheng. To evaluate the performance of the CALPUFF model, the simulated concentrations were compared with the observational data at three monitoring stations. The results show that the CALPUFF simulation results underestimate the daily average concentrations of $PM_{2.5}$, and the statistical analysis also reveals an underestimation trend.

According to the results of the CALPUFF model, in most areas of Jincheng, the range of the highest 24-h primary $PM_{2.5}$ concentrations is 15–120 μg/m^3 in July and 15–240 μg/m^3 in December. Primary $PM_{2.5}$ concentrations in December are significantly higher than those in July. However, the concentrations of secondary SO_4^{2-} and NO_3^- in July are higher than those in December. The concentrations of primary $PM_{2.5}$ decrease gradually outward from the Jincheng city center. From the analysis of the source contributions of the $PM_{2.5}$ concentration, the contribution of residential heating is the largest in December, accounting for 50%. The contributions of industrial processes and dust are significant for the $PM_{2.5}$ concentration, accounting for 18% and 14%, respectively. However, the analysis of the $PM_{2.5}$ concentration contribution may not be sufficiently accurate due to the limitations of the source inventory, but it could be beneficial for the reduction in $PM_{2.5}$ emissions..

Credit author statement

We have made substantial contributions to conception or design of the work; or the acquisition, analysis, or inter pretation of data for work; and we have drafted the work or revised it critically for important intellectual content; and we have approved the final version to be published; and we agree to be accountable for all aspects to the work in ensuring that questions related to the accuracy or integrity of any part of the work are appropriately investigated and resolved.

All persons who have made substantial contributions to the work reported in the manuscript, including those who provided editing and

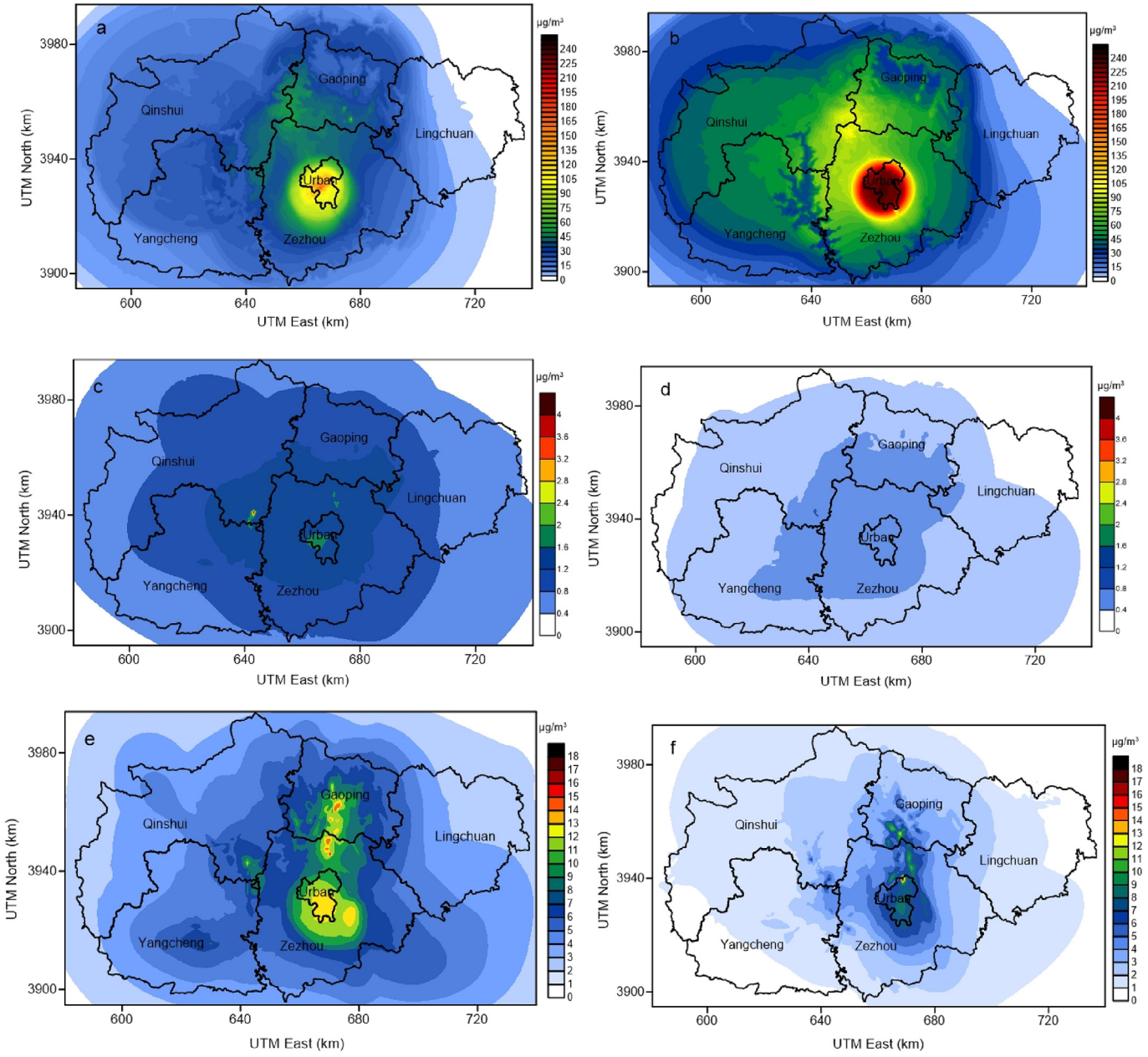

Fig. 5. The spatial distributions of primary $PM_{2.5}$ (a and b), secondary SO_4^{2-} (c and d) and secondary NO_3^- (e and f) in July (left) and December (right).

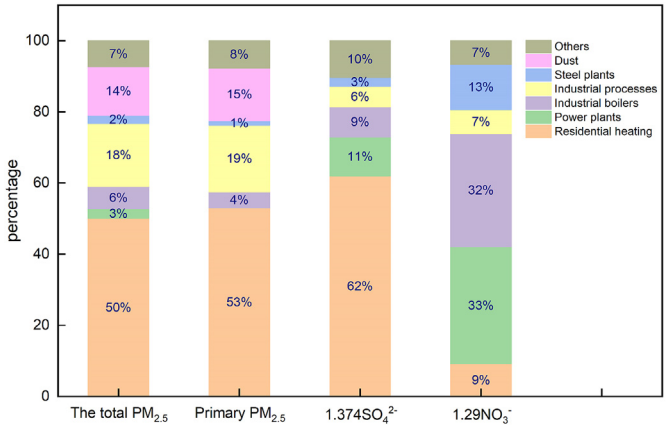

Fig. 6. The source contributions of $PM_{2.5}$ concentrations (Others include: cement plants, coking plants, etc.).

writing assisstance but who are not authors, are named in the Acknowledgments section of the manuscript and have given their written permission to be named. If the manuscript does not include Achnowledgments, it is because the authors have not received substantial contributions form nonauthors.

Declaration of competing interest

The authors declared that they have no conflicts of interest to this work. We declare that we do not have any commercial or associative interest that represents a conflict of interest in connection with the work submitted.

References

Abdul-Wahab, S., Fadlallah, S., Al-Rashdi, M., 2018. Evaluation of the impact of ground-level concentrations of SO_2, NO_x, CO and PM_{10} emitted from a steel melting plant on Muscat, Oman. Sustain Cities Soc 38, 675–683.

Abdul-Wahab, S.A., Fadlallah, S.O., 2014. A study of the effects of vehicle emissions on the atmosphere of Sultan Qaboos University in Oman. Atmos. Environ. 98, 158–167.
Arunachalam, S., Wang, B., Davis, N., Baek, B.H., Levy, J.I., 2011. Effect of chemistry-transport model scale and resolution on population exposure to $PM_{2.5}$ from aircraft emissions during landing and takeoff. Atmos. Environ. 45, 3294–3300.
Cai, B.F., Wang, J.N., Long, Y., Li, W.X., Liu, J.G., Ni, Z., Bo, X., Li, D., Wang, J.H., Chen, X.J., Gao, Q.X., Zhang, L.X., 2015. Evaluating the impact of odors from the 1955 landfills in China using a bottom-up approach. J. Environ. Manag. 164, 206–214.
CALPUFF Dispersion Model (ver.5) – a User's Guide. Earth Tech Inc, Concord, MA,USA.
Choi, G.S., Lim, J.M., Lim, K.S.S., Kim, K.H., Lee, J.H., 2018. Characteristics of regional scale atmospheric dispersion around Ki-Jang research reactor using the Lagrangian Gaussian puff dispersion model. Nucl Eng Technol 50, 68–79.
Cui, H.L., Yao, R.T., Xu, X.J., Xin, C.T., Yang, J.M., 2011. A tracer experiment study to evaluate the CALPUFF real time application in a near-field complex terrain setting. Atmos. Environ. 45, 7525–7532.
Ghannam, K., El-Fadel, M., 2013. Emissions characterization and regulatory compliance at an industrial complex: an integrated MM5/CALPUFF approach. Atmos. Environ. 69, 156–169.
Hanna, S.R., Egan, B.A., Purdum, J., Walgler, J., 2001. Evaluation of the ADMS, AERMOD, and ISC3 dispersion models with the OPTEX, duke forest, kincaid, indianapolis and lovett field datasets. Int. J. Environ. Pollut. 16, 1–6.
Hoinaski, L., Franco, D., Lisboa, H.D.M., 2016. Comparison of plume lateral dispersion coefficients schemes: effect of averaging time. Atmos Pollut Res 7, 134–141.
Holnicki, P., Kałuszko, A., Trapp, W., 2016. An urban scale application and validation of the CALPUFF model. Atmos Pollut Res 7 (3), 393–402.
Jain, R., Vaughan, J., Heitkamp, K., Ramos, C., Claiborn, C., Schreuder, M., Schaaf, M., Lamb, B., 2007. Development of the ClearSky smoke dispersion forecast system for agricultural field burning in the Pacific Northwest. Atmos. Environ. 41, 6745–6761.
Jincheng Environmental Protection Department, 2017. Jincheng's 2017 Pollution Source Emission Inventory.
Kalhor, M., Bajoghli, M., 2017. Comparison of AERMOD, ADMS and ISC3 for incomplete upper air meteorological data (case study: steel plant). Atmos Pollut Res 8 (6), 1203–1208.
Lee, H.D., Yoo, J.W., Kang, M.K., Kang, J.S., Jung, J.H., Oh, K.J., 2014. Evaluation of concentrations and source contribution of PM_{10} and SO_2 emitted from industrial complexes in Ulsan, Korea: interfacing of the WRF–CALPUFF modeling tools. Atmos Pollut Res 5, 664–676.
Levy, J.I., Spengler, J.D., Hlinka, D., Sullivan, D., Moon, D., 2002. Using CALPUFF to evaluate the impacts of power plant emissions in Illinois: model sensitivity and implications. Atmos. Environ. 36 (6), 1063–1075.
Li, S.Y., Xie, S.D., 2016. Spatial distribution and source analysis of SO_2 concentration in Urumqi. Int. J. Hydrogen Energy 41, 15899–15908.
Liu, S.T., Zhang, Z.B., Wang, Y., Hu, Y.L., Liu, W.T., Chen, C.M., Mei, Y.Q., Sun, H., 2019. $PM_{2.5}$ emission characteristics of coal-fired power plants in Beijing-Tianjin-Hebei region, China. Atmos Pollut Res 10, 954–959.
Lopez, M.T., Zuk, M., Garibay, V., Tzintzun, G., Iniestra, R., Fernández, A., 2005. Health impacts from power plant emissions in Mexico. Atmos. Environ. 39, 1199–1209.
Macintosh, D.L., Stewart, J.H., Myatt, T.A., Sabato, J.E., Flowers, G.C., Brown, K.W., Hlinka, D.J., Sullivan, D.A., 2010. Use of CALPUFF for exposure assessment in a near-field, complex terrain setting. Atmos. Environ. 44, 262–270.
Mangia, C., Cervino, M., Gianicolo, E.A.L., 2015. Secondary particulate matter originating from an industrial source and its impact on population health. Int. J. Environ. Res. Publ. Health 12, 7667–7681.
Mardones, C., Saavedra, A., &, 2016. Comparison of economic instruments to reduce $PM_{2.5}$ from industrial and residential sources. Energy Pol. 98, 443–452.
Melo, A.M.V.D., Santos, J.M., Mavroidis, I., Junior, N.C.R., 2012. Modelling of odour dispersion around a pig farm building complex usin AERMOD and CALPUFF. Comparison with wind tunnel results. Build. Environ. 56, 8–20.
Mesoscale and Microscale Meteorology Division, National Center for Atmospheric Research, 2005. Weather Research Forecasting Version 3 Modeling System User's Guide. https://www2.mmm.ucar.edu/wrf/users/docs/user_guide_V3/contents.html.
Murena, F., Mocerinob, L., Quarantab, F., Toscanoa, D., 2018. Impact on air quality of cruise ship emissions in Naples, Italy. Atmos. Environ. 187, 70–83.
Nagendra, S.M.S., Diya, M., Chithra, V.S., Menon, J.S., Peter, A.E., 2016. Characteristics of air pollutants at near and far field regions of a national highway located at an industrial complex. Transport Res D-TR E 48, 1–13.
Ozkurt, N., Sari, D., Akalin, N., Hilmioglu, B., 2013. Evaluation of the impact of SO_2 and NO_2 emissions on the ambient air-quality in the Çan–Bayramiç region of northwest Turkey during 2007–2008. Total Environ 456– 457, 254–266.
Pivato, A., Barausse, A., Zecchinato, F., Palmeri, L., Raga, R., Lavagnolo, M.C., Cossu, R., 2015. An integrated model-based approach to the risk assessment of pesticide drift from vineyards. Atmos. Environ. 111, 136–150.
Ranzato, L., Barausse, A., Mantovani, A., Pittarello, A., Benzo, M., Palmeri, L., 2012. A comparison of methods for the assessment of odor impacts on air quality: field inspection (VDI 3940) and the air dispersion model CALPUFF. Atmos. Environ. 61, 570–579.
Rood, A.S., 2014. Performance evaluation of AERMOD, CALPUFF, and legacy air dispersion models using the Winter Validation Tracer Study dataset. Atmos. Environ. 89, 707–720.
Sari, D., Bayram, A., 2014. Quantification of emissions from domestic heating in residential areas of İzmir, Turkey and assessment of the impact on local/regional air-quality. Total Environ 488–489, 429–436.
Scire, J.S., Strimaitis, D.G., Yamartino, R.J., 2000. A User's guide for the CALPUFF dispersion model. Earth Tech, Inc. http://www.src.com/calpuff/download/CALPUFF_UsersGuide.pdf.
Tartakovsky, D., Stern, E., Broday, D.M., 2016. Comparison of dry deposition estimates of AERMOD and CALPUFF from area sources in flat terrain. Atmos. Environ. 142, 430–432.
Tartakovsky, D., Stern, E., Broday, D.M., 2016. Dispersion of TSP and PM_{10} emissions from quarries in complex terrain. Total Environ 542, 946–954.
Tian, H.Z., Qiu, P.P., Cheng, K., Gao, J.J., Lu, L., Liu, K.Y., Liu, X.G., 2013. Current status and future trends of SO_2 and NO_x pollution during the 12th FYP period in Guiyang city of China. Atmos. Environ. 69, 273–280.
US EPA, 1998. Interagency Workgroup on Air Quality Modeling (IWAQM) Phase 2 Summary Report and Recommendations for Modeling Long Range Transport Impacts.
Wang, Y.F., Chen, S.M., Yao, J.M., 2019. Impacts of deregulation reform on $PM_{2.5}$ concentrations: a case study of business registration reform in China. J. Clean. Prod. 235, 1138–1152.
Who, et al., 2006. Who Air Quality Guidelines for Particulate Matter, Ozone, Nitrogen Dioxide and Sulfur Dioxide: Global Update 2005: Summary of Risk Assessment.
Yang, Q.Q., Dai, Q., Han, D.W., Chen, Y.H., Zhang, S.L., 2019. Sensitivity analysis of raindrop size distribution parameterizations in WRF rainfall simulation. Atmos. Res. 228, 1–13.
Yang, X.C., Wu, Q.Z., Zhao, Cheng, H.Q., He, H.J., Ma, Q., Wang, L.N., Luo, H., 2019. New method for evaluating winter air quality: $PM_{2.5}$ assessment using Community Multi-Scale Air Quality Modeling (CMAQ) in Xi'an. Atmos. Environ. 211, 18–28.
Yates, S.R., Ashworth, D.J., Zhang, Q., 2017. Effect of surface application of ammonium thiosulfate on field-scale emissions of 1,3-dichloropropene. Total Environ 58, 316–323.
Yim, S.H.L., Fung, J.C.H., Lau, A.K.H., 2010. Use of high-resolution MM5/CALMET/CALPUFF system: SO_2 apportionment to air quality in Hong Kong. Atmos. Environ. 44, 4850–4858.
Zhou, Y., Levyb, J.I., Hammitt, J.K., Evans, J.S., 2003. Estimating population exposure to power plant emissions using CALPUFF: a case study in Beijing, China. Atmos. Environ. 37, 815–826.
Zhou, Y., Levyb, J.I., Evans, J.S., Hammitt, J.K., 2006. The influence of geographic location on population exposure to emissions from power plants throughout China. Environ. Int. 32, 365–373.